$Ca_{31}Sn_{20}$ and Related Compounds: Novel Zintl Phases Containing Dimers and Pentamers of Tin or Lead

Ashok K. Ganguli, Arnold M. Guloy, E. Alejandro Leon-Escamilla, and John D. Corbett*

Ames Laboratory—DOE[1] and Department of Chemistry, Iowa State University, Ames, Iowa 50011

Received March 31, 1993®

The phases $Ca_{31}Sn_{20}$, $Sr_{31}Pb_{20}$, and $Yb_{31}Pb_{20}$ are obtained by allowing the pure elements to react in sealed Ta containers at 1100–1180 °C followed by slow cooling. All are isostructural with $Pu_{31}Pt_{20}$. The structure of $Ca_{31}Sn_{20}$ was redetermined (*I*4/*mcm*, $Z = 4$, $a = 12.5267(5)$ Å, $c = 39.912(7)$ Å, $R/R_w = 3.2\%/3.7\%$). A new description of the structure is given in terms of isolated tin atoms plus well-bonded tin dimers and linear pentamers (d(Sn–Sn) = 3.06–3.16 Å) in proportions of 5:5:1 within a rather distorted W_5Si_3-like framework. Assignment of classical two-center bonds to the Sn–Sn interactions shows that the compound is electron-precise, consistent with Zintl–Klemm concepts for a valence compound. The diamagnetic susceptibilities of $Ca_{31}Sn_{20}$ and $Sr_{31}Pb_{20}$ and the semiconducting behavior of $Ca_{31}Sn_{20}$ are in accord with this description.

Introduction

Our interest in polar intermetallic compounds has been intensified by recent results for the Zr–Sb,[2] Zr–Sn,[3,4] La–Ge,[5] Ca–Pb,[6] and Ae–Pn (Ae = alkaline-earth metal, Pn = pnictogen)[7,8] binary (and ternary) systems. We were subsequently attracted to the Ca–Sn system in relation to the nature of the intermetallic phases formed by the alkaline-earth metals with Si, Ge, Sn, and Pb as well as some ternary derivatives. Among the binary calcium compounds, the Ca_5X_3 phases with X = Si, Ge occur in the Cr_5B_3 structure[9] while the related lead phase crystallizes off-stoichiometry in a Mn_5Si_3-like superlattice.[6] Other binary phases in the Ca–Sn system are reported to be Ca_2Sn, $Ca_{31}Sn_{20}$, CaSn, and $CaSn_3$,[10] but no Ca_5Sn_3 is listed, and we have been unsuccessful in further attempts to synthesize a compound with this composition. Ternary 5:3 derivatives in W_5Si_3-like structures have been obtained with Cu or Zn as a third element.[11]

The phase that is competitive with the formation of Ca_5Sn_3 (62.5 atom % Ca) is $Ca_{31}Sn_{20}$ (60.8 atom % Ca), which has been found[12] to have the rare and unusual $Pu_{31}Pt_{20}$ structure.[13] Nothing else appears to be known about the calcium example regarding thermodynamic, bonding, or other physical properties. However, the adjoining phases can be rationalized as classical Zintl phases (valence compounds),[14,15] namely Ca_2Sn (Co_2Si-type,[16] closely related to anti-$PbCl_2$), a semiconductor with an oxidation state of 4– on the isolated tin atoms, and CaSn (CrB-type),[17] in which infinite zigzag chains of two-bonded (2b) Sn^{2-} are isoelectronic with Te.

We sought to examine $Ca_{31}Sn_{20}$ from the same perspective. In order to consider the bonding in this more thoroughly, we repeated the structural refinement of $Ca_{31}Sn_{20}$, since this had been investigated earlier only by film methods ($R = 0.092$).[12] We have also determined some conduction and magnetic properties for $Ca_{31}Sn_{20}$ and have attempted to understand its bonding from the Zintl–Klemm perspective.[14,15] Compounds with the same structure have also been found in the Sr–Pb and Yb–Pb systems.

Experimental Section

Synthesis. $Ca_{31}Sn_{20}$, $Sr_{31}Pb_{20}$, and $Yb_{31}Pb_{20}$ were synthesized from the pure elements: Ca and Sr (99.99%, APL Engineered Materials), Eu and Yb (99.95% total, Ames Laboratory), Sn granules (99.99%, Baker analyzed), and Pb granules (99.99%, Aesar). The metals and the reaction products were stored and handled only in helium- or nitrogen-filled gloveboxes. Stoichiometric amounts of Ca and Sn were first loaded into a Ta tube that was then welded under a helium atmosphere. This was in turn jacketed within an evacuated fused silica container that was well-baked prior to sealing in order to remove traces of moisture. Good yields (~85–90%) were obtained after the assembly had been heated in a resistance furnace at 1180 °C for 24 h and then quenched to room temperature, with Ca_2Sn and CaSn as the other components. Annealing the quenched material at 1000–1050 °C for ~2 weeks gives comparable results. Slow cooling from 1180 °C gave suitable monocrystals for diffraction. The current phase diagram[10] suggests that the maximum congruent melting point occurs for Ca_2Sn at or above 1135 °C, although the structural report[12] indicated that $Ca_{31}Sn_{20}$ forms peritectically near 1156 °C. Reaction of the elements in a 5:3 proportion only at ~875 °C gave comparable results, although this produced Ca_2Sn and an unknown product when the reaction was subsequently equilibrated at 1050 °C and the mixture cooled slowly, the last temperature being below the reported $Ca_{31}Sn_{20}$ peritectic.

Nearly single-phase samples of $Sr_{31}Pb_{20}$ and $Yb_{31}Pb_{20}$ were obtained after the appropriate mixture of elements in welded Ta containers had been heated under dynamic vaccum at 1100 °C for 2–10 h, followed by slow cooling (13 °C/h) to 650 °C. A $Ca_{31}Sn_{20}$ sample gave the equivalent result. The dynamic vacuum conditions were used in order to remove hydrogen (invariably present in alkaline-earth metals[8]), but this impurity turns out to have not influence on these particular compounds. The structure does not appear to form in Ca–Pb, Sr–Sn, Ba–Sn,Pb, Eu–Sn, Eu–Pb, or Yb–Sn systems. The cell dimensions of the new examples $Sr_{31}Pb_{20}$ and $Yb_{31}Pb_{20}$ are respectively $a = 13.2839(7)$, $12.5270(8)$ Å and $c = 42.704(4)$, $40.453(4)$ Å. The impurity oxide phase in Ca–Sn is the anti-perovskite ($Pm\bar{3}m$) Ca_3SnO ($a = 4.831$ (1) Å) as already known for Ca_3PbO.[18]

* Abstract published in *Advance ACS Abstracts*, September 1, 1993.
(1) Ames Laboratory is operated for the U.S. Department of Energy by Iowa State University under Contract No. W-7405-Eng-82. This research was supported by the Office of the Basic Energy Sciences, Materials Sciences Division, DOE.
(2) Garcia, E.; Corbett, J. D. *Inorg. Chem.* **1990**, *29*, 3274.
(3) Kwon, Y.-U.; Corbett, J. D. *Chem. Mater.* **1992**, *4*, 1348.
(4) Kwon, Y.-U.; Sevov, S. C.; Corbett, J. D. *Chem. Mater.* **1990**, *2*, 550.
(5) Guloy, A. M.; Corbett, J. D. *Inorg. Chem.* **1993**, *32*, 3532.
(6) Guloy, A. M. Ph.D. Dissertation, Iowa State University, 1992.
(7) Hurng, W.-M.; Corbett, J. D. *Chem. Mater.* **1989**, *1*, 311.
(8) Leon-Escamilla, E. A.; Corbett, J. D. Unpublished research.
(9) Eisenmann, B.; Schäfer, H. *Z. Naturforsch.* **1974**, *B29*, 460.
(10) *Binary Alloy Phase Diagrams*, 2nd ed.; Massalski, T., Ed.; American Society for Metals International: Metal Park, OH, 1990.
(11) Ganguli, A. K.; Corbett, J. D. To be published.
(12) Fornasini, M. L.; Franceschi, E. *Acta Crystallogr.* **1977**, *33B*, 3476.
(13) Cromer, D. T.; Larson, A. C. *Acta Crystallogr.* **1977**, *33B*, 2620.
(14) Schäfer, H. *Annu. Rev. Mater. Sci.* **1985**, *15*, 1.
(15) Klemm, W.; Busmann, E. *Z. Anorg. Allg. Chem.* **1963**, *319*, 297.
(16) Echerlin, P.; Leicht, E.; Wölfel, E. *Z. Anorg. Allg. Chem.* **1961**, *307*, 145.
(17) Echerlin, P.; Meyer, H. J.; Wölfel, E. *Z. Anorg. Allg. Chem.* **1955**, *281*, 322.
(18) Widera, A.; Schäfer, H. *Mater. Res. Bull.* **1980**, *15*, 1805.

0020-1669/93/1332-4349$04.00/0

Table I. Selected Data Collection and Refinement Parameters for $Ca_{31}Sn_{20}$

lattice params, Å[a]	a = 12.5267(5), c = 39.912(7)
V, Å^3	6263(2)
space group, Z	$I4/mcm$ (No. 140), 4
μ, cm^{-1} (Mo Kα)	103.5
transm coeff range	0.769–1.075
no. of ind obs refl, variables	835, 75
R_{av}(all data), R_{av}(obs)	0.12, 0.039
R, R_w[b]	0.032, 0.033

[a] Guinier data with Si as an internal standard, λ = 1.540 562 Å. [b] $R = \sum||F_o| - |F_c||/\sum|F_o|$; $R_w = [\sum w(|F_o| - |F_c|)^2/\sum w(F_o)^2]^{1/2}$; $w = \sigma_F^{-2}$.

Table II. Positional Parameters and B_{eq} Values for $Ca_{31}Sn_{20}$[a]

atom	x	y	z	B_{eq},[b] Å^2
Ca1	0	$^1/_2$	$^1/_4$	0.9(2)
Ca2	0	$^1/_2$	0.0740(1)	1.5(1)
Ca3	0	$^1/_2$	0.1627(1)	1.6(1)
Ca4	0.1659(4)	$x + ^1/_2$	0	1.6(1)
Ca5	0.2889(3)	0.4445(2)	0.05258(7)	1.3(1)
Ca6	0.2888(3)	0.5779(3)	0.13702(7)	1.3(1)
Ca7	0.2854(2)	0.4147(3)	0.21215(7)	1.4(1)
Sn1	0	0	0	1.62(7)
Sn2	0	0	$^1/_4$	0.99(6)
Sn3	0	0	0.09426(5)	1.38(5)
Sn4	0	0	0.17315(5)	0.91(4)
Sn5	0.4135(1)	$x + ^1/_2$	0	1.03(4)
Sn6	0.19846(8)	$x + ^1/_2$	0.07490(3)	1.13(3)
Sn7	0.3388(1)	$x + ^1/_2$	0.12368(3)	1.26(3)
Sn8	0.15324(8)	$x + ^1/_2$	0.20862(4)	1.13(3)

[a] The positional parameters are identified as for $Pu_{31}Pt_{20}$.[13] [b] $B_{eq} = (8\pi^2/3)\sum_i\sum_j U_{ij}a_i^*a_i^*\vec{a}_i\cdot\vec{a}_j$.

Powder X-ray Diffraction. Powder patterns were obtained on powdered samples mounted between pieces of cellophane tape. An Enraf-Nonius Guinier camera, Cu Kα_1 radiation, and NBS (NIST) silicon as an internal standard were employed. The known 2θ values of the standard lines were fitted to a quadratic in their position on the film, and lattice constants of the sample were then calculated by a least-squares fit to indexed 2θ data.

Single-Crystal Structure Study. A black platelike crystal with dimensions 0.2 × 0.1 × 0.07 mm was mounted on a glass capillary inside the glovebox. The crystal was first checked by oscillation photographs and then mounted on a CAD-4 automatic diffractometer for data collection with monochromated Mo Kα radiation. Some details of the data collection and refinement are listed in Table I. The diffraction data were corrected for Lorentz and polarization effects and for absorption with the aid of the average of three ψ scans at different θ values. An empirical absorption correction with DIFABS[19] was latter applied before the final anisotropic refinement.

The centrosymmetric space group $I4/mcm$ was indicated on the basis of systematic absences, the $N(Z)$ test, and the Laue group selection. Direct methods (SHELXS[20]) quickly located all Sn atoms and some of the Ca atoms. A few cycles of least-squares refinement and subsequent difference-Fourier synthesis revealed the remaining atoms. No significant deviations from full occupancy of all sites were evident. The final cycle of full-matrix least-squares refinement with 835 observed reflections ($I > 3\sigma_I$) and 75 variables (all positional and anisotropic thermal parameters, Table II) converged at R/R_w = 0.032/0.033. All calculations were performed using the TEXSAN package.[21] The refinement gives one more significant figure in the atom positions and a 3–10-fold drop in standard deviations relative to the previous study,[12] which utilized one-third as many reflections from film. Sn–Sn distances agree within 0.01 Å while differences in d(Ca–Ca), not surprisingly, range up to 0.3 Å.

Properties. Electrical conductivity data between 150 and 200 K were measured at ~35 MHz by an electrodeless "Q" method,[22] the range being limited because of breakage of the container. Approximately 100 mg of a powdered sample with an average particle diameter of 500 μm was mixed with nearly double the amount of chromatographic Al_2O_3 and sealed under helium in a Pyrex tube. The absolute resistivity values are thought to be accurate within a factor of 3. Magnetic susceptibility samples were held between two silica rods within a close-fitting silica tube. The assembly was evacuated, back-filled with helium, and sealed. Four sets of susceptibilities were measured at 0.1–3.0 T over the range 6–298 K on a Quantum Design SQUID magnetometer. No hysteresis was seen. The raw data were corrected for the susceptibilities of the container and the ion cores.

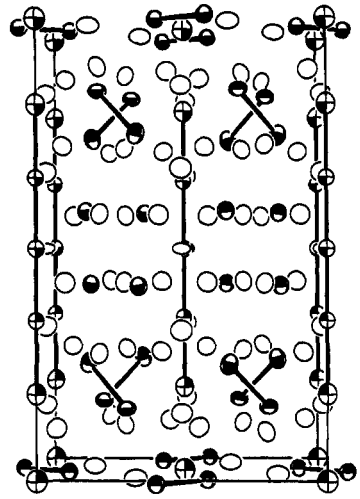

Figure 1. ~[100] view of half of the unit cell of $Ca_{31}Sn_{20}$ with the Sn–Sn bonds emphasized. The Sn and Ca atoms are represented by open and crossed circles, respectively (90% probability thermal ellipsoids).

Results and Discussion

The $Ca_{31}Sn_{20}$ ($Pu_{31}Pt_{20}$) structure has previously been analyzed in terms of a perceived close relationship with the well-studied W_5Si_3 structure.[23] The latter consists of two polyhedral fragments, face-sharing square antiprisms of W1 centered by Si1 that form infinite confacial chains along 0, 0, z and $^1/_2$, $^1/_2$, z and parallel chains of tetrahedral $(Si2)_4W2$ units that share Si edges along 0, $^1/_2$, z etc. The latter silicon atoms also bridge shared antiprism edges on two chains of the first type. Nearly all compounds that crystallize in the W_5Si_3 structure have short M–M bonds between the atoms at the W2 position (0, $^1/_2$, $^1/_4$). The $Ca_{31}Sn_{20}$ ($Pu_{31}Pt_{20}$[13]) structure derives from a 7-fold superstructure of this in $\vec{c}$ in the same space group but with marked perturbations. An alternate geometric description of the W_5Si_3 structure can be given in terms of stacking of 2:1 and 1:1 nets of W and Si, and note has also been made that variants of this basic stacking with some nonplanar nets occur in $Ca_{31}Sn_{20}$.[12] However, the relationships become somewhat distant as one moves from the mirror plane at $z = ^1/_4$ toward $z = 0$ or $^1/_2$. The traditional polyhedral analysis of heteroatom distributions about each atom type misses the particularly interesting and distinctive bonding effects within the Sn (vice-Si) element sublattice, namely, the formation of Sn_2 and Sn_5 oligomers.

A view of one-half of the cell of $Ca_{31}Sn_{20}$ along $\vec{c}$ is given in Figure 1 with the shorter Sn–Sn separations emphasized. (The other half of the cell is generated by a c-glide about (110) or by (002) mirror planes.) The presence of linear Sn_5 pentamers and Sn_2 dimers as well as isolated Sn atoms is striking. The pentamers centered on Sn2 at $z = ^1/_4$ run parallel to the c axis along 0, 0, z and $^1/_2$, $^1/_2$, z. Two kinds of dimers are present, Sn5–Sn5 across cell edges or faces in the (002) planes and Sn6–Sn7 centered at $^1/_4$, $^1/_4$, ~ $^1/_8$ etc. The distances in these (Å) are as follows:

$$Sn3 \overset{3.15}{\text{---}} Sn4 \overset{3.07}{\text{---}} Sn2 \overset{3.07}{\text{---}} Sn4 \overset{3.15}{\text{---}} Sn3$$

$$Sn5 \overset{3.06}{\text{---}} Sn5 \qquad Sn6 \overset{3.16}{\text{---}} Sn7$$

(19) Walker, N.; Stuart, D. *Acta Crystallogr.* **1983**, *A39*, 158.
(20) Sheldrick, G. M. SHELXS-86. Universität Gottingen, BRD, 1986.
(21) TEXSAN, version 6.0 package. Molecular Structure Corp., The Woodlands, TX, 1990.
(22) Shinar, J.; Dehner, B.; Beaudry, B. J.; Peterson, D. T. *Phys. Rev.* **1988**, *B37*, 2066.
(23) Aronsson, B. *Acta Chem. Scand.* **1955**, *9*, 1107.

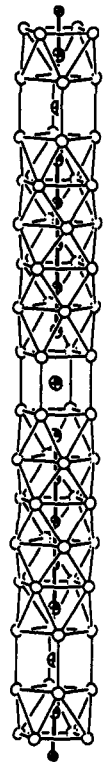

Figure 2. The column of distorted square antiprisms and elongated cubes centered by Sn atoms that lies along 0, 0, z (slightly more than one cell shown). The Sn_5 chains through the center of the antiprismatic position are highlighted. Shaded and open circles represent Sn and Ca atoms, respectively.

These three oligomers and isolated Sn1 + Sn8 atoms occur in proportions of 2:2:8:10 in the half-cell ($Z = 2$). The only other Sn···Sn separation below 4.00 Å is 3.76 for Sn1···Sn3 around what clearly seem to be isolated Sn1 atoms. The genesis of the pentamers starting with a W_5Si_3-like framework is easiest to see; the infinite chains of Sn centered in the confacial antiprisms are progressively distorted with the shift of two adjoining Sn4, Sn3 centers toward the center Sn2 in the layer at $z = {}^1/_4$, leaving the last Sn1 isolated at $z = 0, {}^1/_2$. Further away from this ideal region, the Sn6 and Sn7 atoms that were formerly members of adjoining tetrahedral chains shift toward one another and dimerize. An even greater rearrangement of analogous atoms occurs within the last layer at $z = 0, {}^1/_2$ where Sn5 dimers form. Remnants of the parent structure can be found most clearly in the Ca polyhedra that surround the pentamers (Figure 2). Here pairs of columns built of five face-sharing square antiprisms of Ca5,6,7 in turn stack in an eclipsed fashion in the full cell to create an elongated cube of Ca5 atoms around Sn1 between the five-membered columns.

These changes can be followed best with the [001] sections around $z = 0.25, 0.10$, and 0 shown in Figure 3. The first (Figure 3a) is much more like that of W_5Si_3:[24] square antiprisms of Ca7 about 0, 0, ${}^1/_4$ and ${}^1/_2, {}^1/_2, {}^1/_4$ that are centered by Sn2 and interconnected via edge-bridging Sn8 atoms that are also members of the edge-sharing tetrahedra along $0, {}^1/_2, z$. The next section (Figure 3b) shows the related network around the Sn3 atoms at the ends of the pentamer where the nominal square antiprisms of Ca5,6 around 0, 0, 0.1 and ${}^1/_2, {}^1/_2$, 0.1 have twisted, and Sn6 and Sn7 on neighboring shared edges have folded out of the plane of the antiprism faces to form dimers. Finally, the section around $z = 0, {}^1/_2$ in Figure 3c contains the Sn5 dimers, formerly one edge of shared Si2 tetrahedra along $0, {}^1/_2, z$ that were generated through further twising of the antiprisms and displaced into cavities

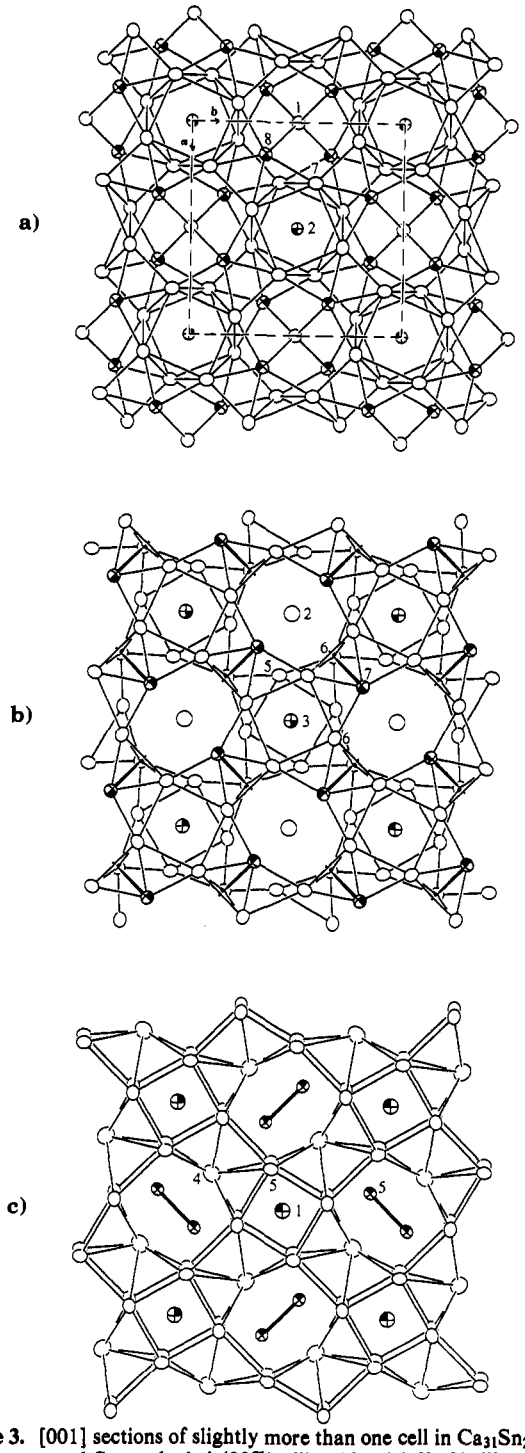

Figure 3. [001] sections of slightly more than one cell in $Ca_{31}Sn_{20}$ with Ca as open and Sn as shaded (90%) ellipsoids: (a) W_5Si_3-like section around $z = 0.25$ (antiprismatic Ca7 and tetrahedral Sn8 columns along $(0, 0, z; {}^1/_2, {}^1/_2, z)$ and $0, 1/2, z$ etc., respectively); (b) distorted structure around $z \sim 0.10$ (twisted Ca5,6 antiprisms centered by Sn3, the end members of the Sn_5 units; edge-bridging Sn6,7 atoms forming dimers); (c) cube-like Ca5 columns centered by isolated Sn1 atoms around $z = 0$ (Ca4 atoms capping side faces of the cubes; Sn5–Sn5 dimers present in the former tetrahedral columns). (The last section has been tilted slightly.)

at 0, ${}^1/_2$, 0 formerly occupied by W2. The destruction of the W_5Si_3-type arrangement at this point is clear. The Ca arrangement is now centered (elongated) cubes at Ca5 atoms plus additional Ca4 atoms that cap side faces on pairs of cubes. Remnants of the tetrahedral chains along $0, {}^1/_2\ z$ etc. in W_5Si_3 that exhibit short W2–W2 distances are retained in this structure but only between $z = 0.07$ and 0.43 (Figure 3a,b). The corresponding Ca1, Ca3, and Ca2 atoms still characteristically

(24) Pearson, W. B. *The Crystal Chemistry and Physics of Metals and Alloys*; Wiley-Interscience: New York, 1972; p 731.

Table III. Bond Distances in $Ca_{31}Sn_{20}$ (Å)

Ca1–Ca3	×2	3.483(6)	Ca7–Ca6	×1	3.796(4)
Ca1–Ca7	×8	4.026(3)	Ca7–Ca7	×1	3.791(6)
Ca1–Sn8	×4	3.178(1)	Ca7–Ca7	×1	3.546(6)
			Ca7–Ca7	×1	3.700(6)
Ca2–Ca3	×1	3.543(8)	Ca7–Ca7	×2	4.090(4)
Ca2–Ca4	×2	4.165(6)	Ca7–Sn1	×1	3.263(3)
Ca2–Ca5	×4	3.783(4)	Ca7–Sn4	×1	3.284(3)
Ca2–Sn5	×2	3.326(5)	Ca7–Sn7	×1	3.974(3)
Ca2–Sn6	×2	3.516(2)	Ca7–Sn8	×1	3.419(3)
Ca2–Sn7	×2	3.478(4)	Ca7–Sn8	×1	3.367(4)
			Ca7–Sn8	×1	3.670(3)
Ca3–Ca1	×1	3.483(6)			
Ca3–Ca2	×1	3.543(8)	Sn1–Sn3	×2	3.762(2)
Ca3–Ca6	×4	3.886(4)	Sn1–Ca5	×8	3.447(3)
Ca3–Ca7	×4	4.221(4)			
Ca3–Sn7	×2	3.254(3)	Sn2–Sn4	×2	3.067(2)
Ca3–Sn8	×2	3.275(4)	Sn2–Ca7	×8	3.263(3)
Ca4–Ca2	×2	4.165(6)	Sn3–Sn1	×1	3.762(2)
Ca4–Ca5	×4	3.804(3)	Sn3–Sn4	×1	3.149(3)
Ca4–Ca5	×4	4.111(6)	Sn3–Ca5	×4	3.200(3)
Ca4–Sn5	×2	3.314(6)	Sn3–Ca6	×4	3.296(3)
Ca4–Sn6	×2	3.045(2)			
			Sn4–Sn2	×1	3.067(2)
Ca5–Ca2	×1	3.783(4)	Sn4–Sn3	×1	3.149(3)
Ca5–Ca4	×1	3.804(3)	Sn4–Ca6	×4	3.167(3)
Ca5–Ca4	×1	4.111(6)	Sn4–Ca7	×4	3.284(3)
Ca5–Ca5	×2	3.867(5)			
Ca5–Ca5	×1	4.134(7)	Sn5–Sn5	×1	3.063(4)
Ca5–Ca5	×1	4.197(5)	Sn5–Ca2	×2	3.326(5)
Ca5–Ca6	×1	3.762(4)	Sn5–Ca4	×2	3.314(5)
Ca5–Sn2	×1	3.447(3)	Sn5–Ca5	×4	3.315(3)
Ca5–Sn3	×1	3.200(3)			
Ca5–Sn5	×1	3.315(3)	Sn6–Sn7	×1	3.158(2)
Ca5–Sn6	×1	3.212(3)	Sn6–Ca2	×1	3.516(2)
Ca5–Sn6	×1	3.493(3)	Sn6–Ca4	×1	3.045(2)
Ca5–Sn7	×1	3.516(3)	Sn6–Ca5	×2	3.493(3)
			Sn6–Ca5	×2	3.212(3)
Ca6–Ca3	×1	3.886(4)	Sn6–Ca6	×2	3.116(3)
Ca6–Ca5	×1	3.762(4)			
Ca6–Ca6	×1	3.738(7)	Sn7–Sn6	×1	3.158(2)
Ca6–Ca6	×2	3.987(5)	Sn7–Ca2	×1	3.478(4)
Ca6–Ca7	×1	3.629(4)	Sn7–Ca3	×1	3.254(3)
Ca6–Ca7	×1	3.796(4)	Sn7–Ca5	×2	3.516(3)
Ca6–Sn3	×1	3.296(3)	Sn7–Ca6	×2	3.370(4)
Ca6–Sn4	×1	3.167(3)	Sn7–Ca6	×2	3.436(3)
Ca6–Sn6	×1	3.116(3)	Sn7–Ca7	×2	3.974(3)
Ca6–Sn7	×1	3.370(4)			
Ca6–Sn7	×1	3.436(3)	Sn8–Ca1	×1	3.178(1)
Ca6–Sn8	×1	3.456(3)	Sn8–Ca3	×1	3.275(4)
			Sn8–Ca6	×2	3.456(3)
Ca7–Ca1	×1	4.026(3)	Sn8–Ca7	×2	3.367(4)
Ca7–Ca3	×1	4.221(4)	Sn8–Ca7	×2	3.419(3)
Ca7–Ca6	×1	3.629(4)	Sn8–Ca7	×2	3.670(3)

exhibit the shortest, though not particularly remarkable Ca–Cadistances of 3.48–3.54 Å. It seems evident that a pseudo-W_5Si_3 structure has undergone marked distortions and some compositional alteration in order to generate recognizable tin pentamers and dimers in $Ca_{31}Sn_{20}$.

The portion of the $Ca_{31}Sn_{20}$ structure represented by the two most distorted sections in Figure 3b,c is in combination very close to the structure of Y_3Ga_2[25] (Gd_3Ga_2-type[26]). Half of the latter structure is virtually identical to that of Figure 3b; the corresponding Ga2 dimer separation of 2.791(3) Å compares with the next shortest distance of 3.70 Å between isolate atoms. This portion likewise shares square faces with $z = 0$ section in Figure 3c except that the pairs of main-group elements are not drawn together in dimers, and yttrium (Gd, W2) atoms still occupy the centers of the channels along $^1/_2$, 0, z etc., as in Figure 3b. This gives a $Y_{24}Ga_{16}$ composition for the two sections in Y_3Ga_2 compared with $Ca_{22}Sn_{16}$ in the present case (where the sections have 2:1 proportions).

We can count the bonding electron requirements of tin as follows if a classical, localized bonding scheme is presumed. Each pentamer contains two singly-bonded Sn3 atoms (1b-Sn^{3-} in oxidation state; compare I_2) and three doubly-bonded Sn2,4 atoms (2b-Sn^{2-}, isoelectronic with Te), which lead to a Sn_5^{12-} formulation. Likewise, each Sn5–Sn5 and Sn6–Sn7 dimer is Sn_2^{6-} and each isolated atom has an oxidation state of Sn^{4-}, corresponding to a filled valence level $5p^6$. There are 4 pentamers, 20 dimers, and 20 isolated tin atoms in the unit cell with a total of −248 oxidation states, exactly opposite that of 124 dipositive Ca atoms per cell. In other words, this striking array of tin aggregates corresponds exactly to that necessary to achieve a valence or Zintl compound. It is virtually impossible to understand the distortions within this structure if they are not driven by Sn–Sn bonding. Of course, one should not expect actual charges to be nearly as high as the assigned oxidation states.

Our assignments of formal, localized, single bonds to Sn–Sn distances of 3.06–3.16 Å are reasonable in comparison with those in other phases that are structurally Zintl types. Sn–Sn distances of 2.967(2) Å are observed for Sn_4^{4-} (T_d) in β-NaSn,[27] 2.94 Å in linear (assigned) Sn_3^{7-} in Li_7Sn_3,[28] 3.00 Å for the assumed Sn_2^{6-} dimers (plus Sn^{4-}) in Li_7Sn_2,[29] and 2.94 Å in SrSn with planar zigzag chains of 2b-Sn^-.[30] There are several factors that affect the observed distances relative to the standard single-bond distance for tin, 2.84 Å[31] (or some other reference). First are bond length increases brought about by charge repulsion within the oligomeric anions; for example, an increase of 0.15–0.20 Å in double-bonded X_4^{2-} species has been estimated for X = Si, Ge with lithium cations.[32] Both cation fields and steric crowding (matrix effects) are also expected to be important. In the present case, the longer Sn5–Sn6 dimer (3.16 Å) correlates very well with the presence of two particularly close pairs of Ca5 and Ca6 around Sn6 positioned such that a bond lengthening would be expected. This is also consistent with the especially short Sn6–Ca4 separation outside this dimer that opposes the lengthening. Longer Sn3–Sn4 distances at the ends of the pentamer also seem to correlate with four short Sn4–Ca6 separations that restrict the Sn4 approach to Sn3. On the other hand, one should not find the shorter Ca···Ca separations (3.48, 3.54 Å) particularly surprising relative to the single-bond distance in the metal, 3.94 Å. A substantial charge transfer from and a shrinkage of calcium is to be expected; compare 3.40 Å in CaO and 3.416(1) Å in Ca_3SnO.

Consistent with the foregoing Zintl phase assignment, $Ca_{31}Sn_{20}$ and $Sr_{31}Pb_{20}$ both exhibit nearly temperature-independent diamagnetism. The magnetic susceptibilities (corrected, in 10^{-4} emu/mol) vary from −6.3 to −4.8 and from −15.2 to −10.2, respectively, between 298 and 20 K. The electrical resistivities of $Ca_{31}Sn_{20}$ are in complete accord: $\rho_{200} \sim 200$ μΩ·cm with a coefficient of −0.36% K^{-1}.

Similar dimer and pentamer formation in $Pu_{31}Pt_{20}$ and $Pu_{31}Rh_{20}$[13] is more difficult to interpret as the compounds are very electron-rich (metallic) when Pu^{3+} is assumed, and it is difficult to judge what degree of valence-shell filling of these oligomers is the appropriate model (≈Au^-, Hg^0, Pb^0?). Direct bonding seems evident. The distances within the pentamers in these are fairly proportional to those in Sn_5^{12-} relative to smaller single-

(25) Zhao, J.-T.; Corbett, J. D. Unpublished research. Y_3Ga_2 etc. are also Zintl phases structurally with equal numbers of isolated and dimerized gallium atoms [$(Y^{3+})_6(Ga^{5-})_2(Ga_2)^{8-}$ in oxidation states], but Y_3Ga_2 is Pauli-paramagnetic with a metal-like coefficient of conductivity.
(26) Yatsenko, S.-P.; Hladyschewsky, R. E.; Sitschewitsh, O. M.; Belsky, V. K.; Semyannikov, A. A.; Hryń, Yu. N.; Yarmolyuk, Ya. P. *J. Less-Common Met.* **1986**, *115*, 17.
(27) Müller, W.; Volk, K. *Z. Naturforsch.* **1977**, *32B*, 709.
(28) Müller, W. *Z. Naturforsch.* **1974**, *29B*, 304.
(29) Frank, U.; Müller, W.; Schäfer, H. *Z. Naturforsch.* **1974**, *30B*, 6.
(30) Widera, A.; Schäfer, H. *J. Less-Common Met.* **1981**, *77*, 29.
(31) Pauling, L. *The Nature of the Chemical Bond*; Cornell University Press: Ithaca, NY, 1960; p 400.
(32) Nesper, R. *Prog. Solid State Chem.* **1990**, *20*, 1.

bond lengths of Pt and Rh.[31] In contrast, the bond lengths in the platinum metal dimers range between the same distance as with tin to 0.07 Å *greater*. The $Pu_{31}X_{20}$ compounds could still qualify as "metallic Zintl phases"[32] in which substantial covalent bonding components lie below a sea of conduction electrons.

Size proportions may be important to the stability of $Ca_{31}Sn_{20}$ since the only other alkaline-earth metal (Ae) analogue we have been able to obtain is $Sr_{31}Pb_{20}$, thus excluding Ca–Pb, Sr–Sn, and Ba–Sn,Pb members. However, extension to the divalent lanthanides Eu and Yb adds $Yb_{31}Pb_{20}$ to the collection, Yb^{2+} being a close size-equivalent of Ca^{2+}. Generalizations are a little dangerous, however, if the alternative, competing phases also change from system to system, as they do in some instances. Even so, regularities therewith are not clear. All nine systems as presently known (Eu–Sn has not been investigated)[10] contain Ae_2X (usually Co_2Si-type) and AeX (CrB or CuAu) phases. In addition, the Sr–Sn, Sr–Pb, Ba–Sn, and Yb–Sn systems also contain Ae_5X_3(Cr_5B_3), yet Sr–Pb still provides $Ae_{31}X_{20}$. (Furthermore, this system also contains an Sr_5Pb_4 (Gd_5Si_4-type) phase as well.) On the other hand, Ca–Sn and Ba–Pb are presently not known to contain any competing phases between 50 and 67% Ca yet only the first gives $Ca_{31}Sn_{20}$. The Yb–Pb system, which includes $Yb_{31}Pb_{20}$, is also reported to form an intermediate Mn_5Si_3-type phase, but that composition is likely not correct, perhaps being instead related to the Ae-rich superstructure found in Ca–Pb.[6] Rationalizations for the occurrence of the three particular $Ae_{31}X_{20}$ phases are not very obvious.

It is fascinating to realize that the Zintl–Klemm concept works as a guide not only for simple structures like those of Ca_2Sn and CaSn but also in such seemingly complicated cases as $Ca_{31}Sn_{20}$.

Acknowledgment. The authors are indebted to J. Ostenson and D. Finnemore for the magnetic data and J. Shinar for the use of the conductivity apparatus.

Supplementary Material Available: Listings of additional data collection and refinement information and anisotropic atom displacement parameters and a stereoview of $Ca_{31}Sn_{20}$ (3 pages). Ordering information is given on any current masthead page.